

Observable consequences of pseudo-complex General Relativity

P. O. Hess^{1,2}

¹ *Instituto de Ciencias Nucleares, Universidad Nacional Autónoma de México,
Circuito Exterior, C.U., A.P. 70-543, 04510 México D.F., Mexico*

² *Frankfurt Institute for Advanced Studies, Johann Wolfgang Goethe Universität,
Ruth-Moufang-Str. 1, 60438 Frankfurt am Main, Germany*

January 13, 2021

Abstract

A review of the *pseudo-complex General Relativity* (pc-GR) is presented, with the emphasis on observational consequences. First it is argued why to use an algebraic extension and why the pseudo-complex is a viable one. Afterward, the pc-GR is formulated. Posterior, several observational consequences are discussed, as the perihelion shift of Mercury, Quasi Periodic Objects, the emission profile of accretion discs, the pc-Robertson-Walker model of the universe, neutron stars and gravitational ring-down modes of a black hole.

1 Introduction

The *General Relativity* (GR) is up to now the most successful theory of Gravitation. Many observations have been confirmed, especially in weak gravitational fields as in the solar system [1]. The existence of gravitational waves were also confirmed [2, 3] and the shadow of a black holes was observed in [4, 5, 6, 7, 8, 9]. Though, the last two observations are related to very strong gravitational fields, we will show that the pc-GR is also able to describe them. The reason lies in the method to deduce masses and distances from the observations, which is based on the assumption that only GR describes the observations.

Attempts to extend GR have a long history [10, 11, 12, 13, 14, 15], all with different motivations. For example, A. Einstein wanted to unify gravity with electrodynamics [10, 11]. On the other hand, M. Born approached a conceptual problem, namely that in Quantum Mechanics coordinates and momenta are treated on an equal footing, while in GR coordinates are predominant. The main motivation for pc-GR [16, 17] was to extend GR via algebraic means and to search for the possibility to eliminate the event-horizon. Why this is important? This depends on the view of the beholder: While some argue that the event horizon is just another coordinate singularity, others complain that from a black hole, even nearby, no information can get out. The no-hair theorem implies that all information is lost, violating fundamental concepts. Also the singularity in its center is bothersome and theories have been proposed [18, 19] to remedy it.

Though, the event horizon is only a coordinate singularity, its origin is the strong gravitational field and there is no reason to believe that GR is still valid. Thus, a search for an extension of GR is justified when the limits of the theory are reached.

In this contribution, we will elaborate on the motivations for proposing the pc-GR and explain its mathematical structure. Apart from presenting a review on the pc-GR, the main body of the text concentrates on observational consequences. Some of the examples were already discussed in earlier publications, but some are new, as will be noted in its course. We will see, that several predictions cannot be distinguished from GR, due to either low resolution, or too small corrections, or alternative explanations within GR. In these cases, one has to wait for further, improved observations.

This contribution is organized as follows: In Section 2 algebraic extensions in general are briefly discussed. In section 3 the pc-GR is resumed. In section 4 the observational predictions and consequences are discussed, which includes: The *Perihelion shift of Mercury*, *Quasi periodic objects*, light emission structure of *accretion discs*, the *pc-Robertson-Walker cosmology*, *neutron stars* and *gravitational ring-down modes* of a black hole. Some of the results were obtained earlier and some are new, as resolving the structure of the pseudo-imaginary part of the coordinates and the perihelion shift of Mercury. In 5 conclusions will be drawn.

The convention $G = c = 1$ is used throughout this contribution, as the metric signature $(- + + +)$

2 Algebraic extensions

A possible option to modify GR is to extend the space-time coordinates x^μ ($\mu = 0, 1, 2, 3$) to a different kind, which is called an *algebraic extension*. The questions to address are: How many algebraic extensions exist? Which of those are consistent with basic principles? If an algebraic extension is consistent was addressed in [20] where all kinds of coordinates were investigated. A more detailed explanation can be found in [21, 22].

Table 1: Algebras of various algebraic coordinate extensions.

Algebra	Generators a_i	algebra
Real	1	-
complex	1, i	$i^2 = -1$
pseudo-complex	1, I	$I^2 = 1$
quaternion	1, a_1, a_2, a_3	$a_i a_j = -\delta_{ij} + \varepsilon_{ijk} a_k$
hyper-quaternions	1, a_1, a_2, a_3	$a_1^2 = a_2^2 = 1,$ $a_1 a_2 = -a_3$

An algebraic extension is defined through the mapping of real coordinates to

$$x^\mu \rightarrow X^\mu = x^\mu + a_i y^\mu \quad (1)$$

where a sum over i is implicit and the a^i satisfy the algebra

$$a_i a_j = C_{ijk} a_k \quad , \quad (2)$$

with a sum of repeated indexes. One example is the complex extension which contains, besides $a_0 = 1$, $a_1 = i$ with $i^2 = -1$. Another one is the pseudo-complex (pc) extension, with the generators $a_0 = 1$ and $a_1 = I$ with $I^2 = 1$. The possible algebras are listed in Table 1.

Several modifications of GR, mentioned in the introduction, are related to algebraic extensions, though not obvious at the first sight. In [22] these attempts were resumed, as the one proposed in [14, 15] which implies a maximal acceleration, or the more obvious one in [23], where the complex extension is proposed.

Most of the algebraic extensions run in a serious problems, when the square of at least one of the a_i is -1. It is shown in [20, 22] that in the limit of nearly flat space the propagator of a gravitational wave has the wrong sign and corresponds to a ghost solution, excluded on physical grounds. Therefore, the main observation of [20] is that apart from the real coordinates, corresponding to GR, the only ones which do not imply ghost and/or Tachyon solutions are the pseudo-complex coordinates. This is a very important finding because it implies that the path through algebraic extensions is only possible through the use of pc-coordinates.

This is the reason why we stick to this extension and in what follows we will expose some consequences, theoretical and observational ones.

3 Pseudo-complex General Relativity

The pc-GR was introduced in [16]. Since then, several reviews were published in [21, 22]. In [17] the theory, their mathematical structure and some observational facts can be retrieved and in [24, 25] some observational predictions were published. One centerpiece in pc-GR is that around any mass vacuum fluctuations accumulate, whose presence is a consequence of semi-classical Quantum Mechanical calculations [26, 27]. These vacuum fluctuations have the nature of a dark energy and semi-classical Quantum Mechanics calculations result in a fall-off of the dark energy density as a function in distance to the mass. Up to now, in pc-GR a *phenomenological ansatz* is used, assuming a fall-off of the dark energy density as $\sim B_n/r^{n+2}$, where B_n describes the coupling of the central mass to the dark energy and r is the radial distance. The n is a parameter, which was assumed to be 3 in [24, 25], because it is the next leading order correction to the metric which still does not contradict solar system observations [1]. However, in [28, 29] it is shown that n has to be > 3 , using the first observed gravitational wave event [2, 3]. For that reason, we assume $n = 4$ in what follows, keeping in mind that this is a *phenomenological assumption*.

One important consequence of the accumulation of dark energy near a central mass is its recoupling to the metric, which is changed such that no event horizon appears. It can rephrased into the principle *that a mass not only curves the space nearby but also changes the vacuum properties*, which may give clues on the quantization of

gravity.

The pc-Gr is formulated in analogy of the GR, using instead of real coordinates x^μ new ones, namely

$$\begin{aligned} X^\mu &= x^\mu + Iy^\mu, \quad I^2 = 1 \\ X^\mu &= X_+^\mu \sigma_+ + X_-^\mu \sigma_- \\ \sigma_\pm &= \frac{1}{2}(1 + I), \quad \sigma_\pm^2 = 1, \quad \sigma_+ \sigma_- = 0, \end{aligned} \quad (3)$$

where two representations are shown, the one in terms of 1 and I and the other one in terms of the so-called *zero-divisor basis*, given by σ_\pm . The σ_\pm behave as projectors, with $(\sigma_\pm)^2 = 1$ and $\sigma_- \sigma_+ = 0$. The last property is important because it allows to perform calculations independently in each zero-divisor component [17].

The metric has also two components and is of the form

$$g_{\mu\nu}(X) = g_{\mu\nu}^+(X_+) \sigma_+ + g_{\mu\nu}^-(X_-) \sigma_- . \quad (4)$$

The length element is defined in terms of X^μ in the same manner as it is defined in terms of x^μ in GR:

$$\begin{aligned} d\omega^2 &= g_{\mu\nu} dX^\mu dX^\nu \\ &= \left\{ g_{\mu\nu}^S [dx^\mu dx^\nu + dy^\mu dy^\nu] + g_{\mu\nu}^A [dx^\mu dy^\nu + dy^\mu dx^\nu] \right\} \\ &\quad + I \left\{ g_{\mu\nu}^A [dx^\mu dx^\nu + dy^\mu dy^\nu] + \right. \\ &\quad \left. g_{\mu\nu}^S [dx^\mu dy^\nu + dy^\mu dx^\nu] \right\} , \end{aligned} \quad (5)$$

with

$$g_{\mu\nu}^S = \frac{1}{2}(g_{\mu\nu}^+ + g_{\mu\nu}^-), \quad g_{\mu\nu}^A = \frac{1}{2}(g_{\mu\nu}^+ - g_{\mu\nu}^-) . \quad (6)$$

We have used the expression of X^μ in terms of x^μ and y^μ for rewriting the length element $d\omega^2$ in (5).

Requiring that particles only move along real distances, a constraint of a *real* length element is imposed, demanding the factor of I in (5) to vanish, i.e.,

$$\begin{aligned}
& (\sigma_+ - \sigma_-) \left\{ g_{\mu\nu}^A [dx^\mu dx^\nu + dy^\mu dy^\nu] + \right. \\
& \left. g_{\mu\nu}^S [dx^\mu dy^\nu + dy^\mu dx^\nu] \right\} = 0 \quad . \quad (7)
\end{aligned}$$

It is illustrative to consider the GR-limit, i.e., $g_{\mu\nu}^A = 0$ and with $g_{\mu\nu}^S = g_{\mu\nu}$ now real, the constriction (7) reduces to

$$g_{\mu\nu} dx^\mu dy^\nu = 0 \quad . \quad (8)$$

This is nothing but the dispersion relation, whose solution is $y^\nu \sim u^\nu$, the four velocity. For dimensional reasons $y^\nu = l u^\nu$, with l a length parameter, related to the *minimal* length of the theory.

Here, it is important to note that pc-GR contains a *minimal length*, which is a mere real number and is not affected by a Lorentz transformation. This simplifies enormously the mathematical structure of the theory, because it does not require a deformation of the Lorentz transformation, needed in theories with a *physical* minimal length. *This observation hints to the alternative to formulate theories which contain a minimal length and still use Lorentz symmetry.*

In general, the solution of (7) is quite complicated and we will discuss two of those in an approximate manner: For the pc-Schwarzschild case and for the pc-Robertson-Walker metric.

The action within pc-GR is defined in analogy to GR, namely

$$S = \int dX^4 \sqrt{-g} (\mathcal{R} + 2\alpha) \quad , \quad (9)$$

where \mathcal{R} is the pc-Riemann scalar, defined in the same way as in GR, and α is a pc-constant for the pc-Robertson-Walker model and may depend on the radial distance for the Schwarzschild case. Note, that also the volume element is pseudo-complex.

Varying this action in each zero-divisor sector, using the constraint (7), leads to the equations of motion

$$\mathcal{R}_{\mu\nu}^\pm - \frac{1}{2} g_{\mu\nu}^\pm \mathcal{R}_\pm = 8\pi T_{\pm \mu\nu}^\Lambda \quad (10)$$

in each zero-divisor basis. The Λ refers intentionally to its property as a dark energy.

The $T_{\pm}^{\Lambda}{}_{\mu\nu}$ is given by

$$8\pi T_{\pm}^{\Lambda}{}_{\mu\nu} = \lambda u_{\mu}u_{\nu} + \lambda(\dot{y}_{\mu}\dot{y}_{\nu} \pm u_{\mu}\dot{y}_{\nu} \pm u_{\nu}\dot{y}_{\mu}) + \alpha g_{\mu\nu}^{\pm} \quad , \quad (11)$$

which can be rewritten such that its property as a, in general, anisotropic fluid is obvious. For that, we refer to [21, 22].

When $T_{\pm}^{\Lambda}{}_{\mu\nu}$ is mapped to the real part, one obtains

$$8\pi T_{\mu\nu}^{\Lambda} = \lambda u_{\mu}u_{\nu} + \lambda\dot{y}_{\mu}\dot{y}_{\nu} + \alpha g_{\mu\nu}^{\pm} \quad . \quad (12)$$

As we will see further below, the y_{μ} can be written as being proportional to the 4-velocity u_{μ} . This allows us to write the (12) proportional to λ as $\lambda(1 + l^2 A(r)) u_{\mu}u_{\nu}$ (here for a central problem), where l^2 describes the correction due to the $\dot{y}_{\mu}\dot{y}_{\nu}$ term. The $A(r)$ can be very large near the event-horizon, as will be seen later.

For the T_{00} -component this implies pc-corrections to the density of the dark energy proportional to l^2 . This effect was already studied in [30], where the effective potential deduced there produces a repulsive potential near the event horizon.

Though, we will discuss some solutions, at the end it will be more effective to assume a *phenomenological approach*, with a specific r -dependence of the dark energy density.

For the dark energy density we prefer to use a phenomenological ansatz, namely

$$\varrho_{\Lambda} \sim \frac{1}{r^{n+2}} \quad . \quad (13)$$

The value of n has to be larger than 3, as discussed earlier. The proportionality factor parametrizes the coupling of the central mass to the dark energy.

After these general consideration, we resume the metric of a rotating star (Kerr metric), which was derived in [24]:

$$g_{00} = -\frac{r^2 - 2m_0 r + a^2 \cos^2 \vartheta + \frac{B_n}{(n-1)(n-2)r^{n-2}}}{r^2 + a^2 \cos^2 \vartheta} \quad ,$$

$$g_{11} = \frac{r^2 + a^2 \cos^2 \vartheta}{r^2 - 2m_0 r + a^2 + \frac{B_n}{(n-1)(n-2)r^{n-1}}} \quad ,$$

$$\begin{aligned}
g_{22} &= r^2 + a^2 \cos^2 \vartheta \quad , \\
g_{33} &= (r^2 + a^2) \sin^2 \vartheta + \frac{a^2 \sin^4 \vartheta \left(2m_0 r - \frac{B_n}{(n-1)(n-2)r^{n-2}} \right)}{r^2 + a^2 \cos^2 \vartheta} \quad , \\
g_{03} &= \frac{-a \sin^2 \vartheta \left(2m_0 r + a \frac{B_n}{(n-1)(n-2)r^{n-2}} \right) \sin^2 \vartheta}{r^2 + a^2 \cos^2 \vartheta} \quad .
\end{aligned} \tag{14}$$

The B_n and a are the above mentioned coupling parameter of the mass to the dark energy and the Kerr rotational parameter, respectively. In what follows $n = 4$ will be assumed and (14) reduces to the standard Kerr solution of GR when $B_n = 0$.

For $n = 4$ and $b_n = \frac{81}{8}$ there is still for $a = 0$ an event horizon at $\frac{3}{2}m_0$. Thus, if we want to eliminate completely this horizon, the value of b_n has to be at least infinitesimal larger than $\frac{81}{8}$. For practical reasons b_n is assumed to acquire the value $\frac{81}{8}$. In that case, a mass function $m(r)$ can be defined, namely

$$m(r) = \left(1 - \frac{27}{32} \left(\frac{m_0}{r} \right)^3 \right) \quad . \tag{15}$$

For the pc-Schwarzschild case the g_{00} component acquires the form $g_{00} = \left(1 - \frac{2m(r)}{r} \right)$, which clearly reduces to the well known expression in GR, when term proportional to $1/r^3$ in $m(r)$ is eliminated.

3.1 Group theoretical properties of the pseudo-complex description

A more complete explanation of the group theoretical structure of the pc-coordinates and their importance in field theory can be found in [17, 31, 32, 33, 34].

The pc-Lorentz transformation is

$$e^{-\omega^{\mu\nu} L_{\mu\nu}} = e^{-\omega_+^{\mu\nu} L_{\mu\nu}^+} \sigma_+ + e^{-\omega_-^{\mu\nu} L_{\mu\nu}^-} \sigma_- \quad , \tag{16}$$

where $L_{\mu\nu}^\pm$ is the generator of the Lorentz group $SO_\pm(3, 1)$, restricted to the \pm zero-divisor component. Its explicit form is given by ($\hbar = 1$)

$$L_{\mu\nu} = X_\mu P_\nu - X_\nu P_\mu$$

$$\begin{aligned}
&= \left(X_\mu^+ P_\nu^+ - X_\nu^+ P_\mu^+ \right) \sigma_+ + \left(X_\mu^- P_\nu^- - X_\nu^- P_\mu^- \right) \sigma_- \\
&= L_{\mu\nu}^+ \sigma_+ + L_{\mu\nu}^- \sigma_-
\end{aligned}$$

with

$$P_\mu = \frac{1}{i} \frac{\partial}{\partial X^\mu} \quad . \quad (17)$$

With this and $[X^\mu, P_\nu] = i\delta_{\mu\nu}$, the commutation relations of the pc-Lorentz transformation generators are [17]

$$[L_{\mu\nu}, L_{\lambda\delta}] = i(g_{\lambda\nu}L_{\delta\mu} + g_{\delta\mu}L_{\lambda\nu} + g_{\lambda\mu}L_{\nu\delta} + g_{\delta\nu}L_{\mu\lambda}) \quad . \quad (18)$$

Thus, the group structure is

$$SO_{pc}(3,1) = SO_+(3,1) \otimes SO_-(3,1) \supset SO(3,1) \quad , \quad (19)$$

i.e., the direct product of two Lorentz groups. This direct product reduces to the standard Lorentz group, when the real part of the pc-generators is projected.

In conclusion, the mathematical structure is very similar to the standard formulation, it only involves twice as much generators and parameters for the transformation, a reflection of the 8-dimensional coordinate space.

4 Observational predictions

In this section, some older, with additions, and some new predictions of the pc-GR are presented. First of all, the general properties of pc-GR related to the y^μ -components are discussed. As mentions above, the y_μ variables can be identified, for the case of a flat space, by lu_μ , where the l is a length parameter introduced for dimensional reasons. An allowed ansatz for a general case is

$$y_\mu = A(x, y)lu_\mu \quad , \quad (20)$$

where $A(x, y)$ is a function in x_ν and y_ν , yet to be determined, where y_μ has the same tensorial properties as u_μ and $A(x, y)$ is a scalar. That (20) is correct will be seen in two examples to be discussed in this paper, namely for the pc-Schwarzschild solution and for the pc-Robertson-Walker metric.

4.1 A general equation for y_μ

In what follows, the general structure is discussed and an equation for the determination of (20) is presented. At the end, the y_μ is obtained within an approximation for the Schwarzschild case, the first example.

A curve in the pseudo-complex manifold is described by the pc-4-vector

$$V^\mu = \frac{dX^\mu}{ds} = \frac{dX_+^\mu}{ds}\sigma_+ + \frac{dX_-^\mu}{ds}\sigma_- \quad , \quad (21)$$

with "s" as the curve parameter, which is the same in both zero-divisor components.

In addition to the pc-coordinates X^μ the *local* coordinates (or co-moving frame) \tilde{X}^μ at a given point p are defined in analogy as

$$X_\pm^\mu = x^\mu \pm y^\mu \quad , \quad \tilde{X}_\pm^\mu = \tilde{x}^\mu \pm \tilde{y}^\mu \quad . \quad (22)$$

Transforming (21) into the co-moving frame in both components, we obtain

$$\frac{dX^\mu}{ds} = e_+^\mu{}^i \frac{d\tilde{X}_+^i}{ds}\sigma_+ + e_-^\mu{}^i \frac{d\tilde{X}_-^i}{ds}\sigma_- \quad , \quad (23)$$

where $e_\pm^i{}_\mu$ ($i=0,2,3,4$) are the inverse matrix elements of $e_\pm^\mu{}_i$. In this contribution only diagonal metrics are discussed, therefore the $e_\pm^i{}_\mu$ are the square roots of the diagonal metric elements.

In a co-moving frame the space is locally flat and, as we saw earlier, the \tilde{y}^μ assume the relation $l\frac{d\tilde{x}^\mu}{ds}$, i.e., it is proportional to the 4-velocity. This results into a relation of the zero divisor components of X^μ in the local frame to x^μ and y^μ :

$$\begin{aligned} \frac{d\tilde{X}_+^i}{ds} &= e_+^i{}_\mu \frac{dX_+^\mu}{ds} = \frac{d\tilde{x}^i}{ds} + \frac{d\tilde{y}^i}{ds} = \left(\frac{1}{l}\right)\tilde{y}^i + \frac{d\tilde{y}^i}{ds} \\ \frac{d\tilde{X}_-^i}{ds} &= e_-^i{}_\mu \frac{dX_-^\mu}{ds} = \frac{d\tilde{x}^i}{ds} - \frac{d\tilde{y}^i}{ds} = \left(\frac{1}{l}\right)\tilde{y}^i - \frac{d\tilde{y}^i}{ds} \quad . \quad (24) \end{aligned}$$

Next, we solve for \tilde{y}^μ and its derivative with respect to s , giving

$$\begin{aligned}
\tilde{y}^i &= l \left[\frac{1}{2} e_{+ \mu}^i \frac{dX_+^\mu}{ds} + \frac{1}{2} e_{- \mu}^i \frac{dX_-^\mu}{ds} \right] \\
\frac{d\tilde{y}^i}{ds} &= \frac{1}{2} e_{+ \mu}^i \frac{dX_+^\mu}{ds} - \frac{1}{2} e_{- \mu}^i \frac{dX_-^\mu}{ds} .
\end{aligned} \tag{25}$$

In a subsequent step, the first equation in (25) is derived further with respect to the line element s and the result is set equal to the second equation in (25). Then, all expression of the σ_+ and σ_- components are collected on one side of the equation, resulting into

$$\begin{aligned}
&l \frac{de_{- \mu}^i}{ds} \frac{dX_-^\mu}{ds} + e_{- \mu}^i \left[l \frac{d^2 X_-^\mu}{ds^2} + \frac{dX_-^\mu}{ds} \right] \\
&- e_{+ \mu}^i \left[\frac{dX_+^\mu}{ds} - l \frac{d^2 X_+^\mu}{ds^2} \right] + l \frac{de_{+ \mu}^i}{ds} \frac{dX_+^\mu}{ds} = 0 .
\end{aligned} \tag{26}$$

Let us consider, as a special case, a central and static problem: Set $dX_\pm^0 = 0$ and $dX_\pm^\vartheta = 0$, $dX_\pm^\varphi = 0$. As an approximation, all terms proportional to the minimal length are neglected compared to the others, because we will not work in the regime of maximal acceleration. We also rescale, for this particular example, the mass parameter to $m_0 = 1$.

The 4-bein tensors $e_{\pm \mu}^i$ are used, restricting to the pure r part:

$$e_{\pm \mu}^i \rightarrow e_{\pm r}^r = 1 - \frac{2m_\pm(X_\pm^r)}{X_\pm^r}, \quad m_\pm = 1 - \frac{27}{32X_\pm^r} . \tag{27}$$

The differential equation (26) then reduces to

$$\frac{dy_r}{dr} = \frac{\left[1 + \frac{27}{16(r-y_r)^4} - \frac{2}{(r-y_r)} \right]^{\frac{1}{2}} - \left[1 + \frac{27}{16(r+y_r)^4} - \frac{2}{(r+y_r)} \right]^{\frac{1}{2}}}{\left[1 + \frac{27}{16(r-y_r)^4} - \frac{2}{(r-y_r)} \right]^{\frac{1}{2}} + \left[1 + \frac{27}{16(r+y_r)^4} - \frac{2}{(r+y_r)} \right]^{\frac{1}{2}}} \tag{28}$$

Furthermore, assuming a small y_r , compared to r , we arrive at

$$\frac{dy_r}{dr} \approx \frac{\left(\frac{27}{8r^5} - \frac{1}{r^2} \right)}{1 + \frac{27}{16r^4} - \frac{2}{r}} y_r . \tag{29}$$

When the differentials dy_r and dr are moved to opposite sides of the equation and we divide it by $d\tau$, where τ is the time parameter, one notes that the time derivative of y_r is proportional to the corresponding component of the four-velocity, as noted further above.

The MATHEMATICA code [35] is used to solve this equation, with the result

$$y_r = A \frac{r^2}{(3-2r)(3+4r+4r^2)^{\frac{1}{2}}} . \quad (30)$$

The integration constant A is determined in the limit of $r \rightarrow \infty$. Requiring that y_r should approach $l\dot{r}_\infty$, leads to $y_r \rightarrow -\frac{A}{4}$, or $A = -4l\dot{r}_\infty$. In this manner, the minimal length l is reintroduced due to the assumed limiting behavior of y_μ .

Thus, the final solution is

$$y_r = \frac{4lr^2}{(2r-3)(3+4r+4r^2)^{\frac{1}{2}}} \dot{r}_\infty . \quad (31)$$

This solution has a pole in $r = \frac{3}{2}$, where y_r tends to $+\infty$ for $r \rightarrow (\frac{3}{2})|_+$. Because we assumed y_r as small compared to r , the solution is not valid anymore near $r = \frac{3}{2}$ and a solution for large y_r has to be found.

Nevertheless, the solution describes the evolution of y_r from large r towards smaller values, when y_r is still small. The limit is when $(2r-3)$ in the denominator is of the order of one, or $r \approx \frac{3}{2} + \frac{l}{2}$, i.e., *very close* to $r = \frac{3}{2}$. A general picture emerges, where y_r is slowly increasing for descending r -values and changes rapidly toward $+\infty$ near $r = \frac{3}{2}$. In Fig. 1 the function y_r/\dot{r}_∞ , in units of the minimal length l , is plotted in the range 1.52 to 2 and, as can be seen, only near 1.5 the curve starts to rise.

4.2 Perihelion shift of Mercury

The first confirmation of General Relativity came from the calculation of the perihelion shift of Mercury. As an illustrative example, in this sub-section, the perihelion shift is investigated, including the pc-corrections, with the modified mass-function $m(r) = m_0 \left(1 - \frac{27}{32} \frac{m_0^3}{r^3}\right)$ (now, we return to $m_0 \neq 1$), where the paths as described in [36]

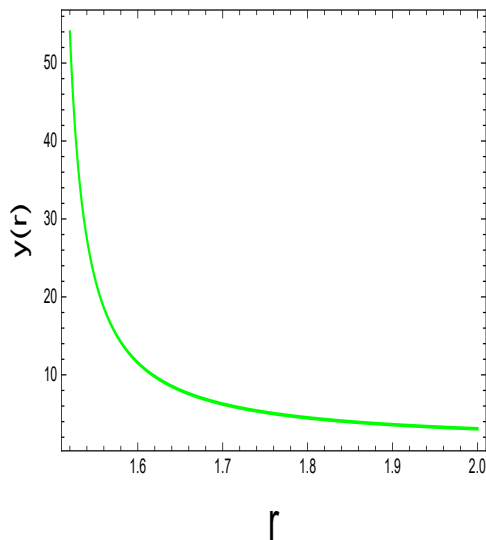


Figure 1: The radial pseudo-imaginary coordinate component $y(r) = y_r/\dot{r}_\infty$ as a function in r . The vertical axis gives $y(r)$ in units of l .

is neatly followed. We will see, that GR gives the dominant contribution, while the additional ones from pc-GR will be too low to be measured. That this correction cannot be measured is not surprising, because the gravitational field in the solar system is simply too weak. The consequences for all other solar system observations are equally small.

The real length element in the pc-Schwarzschild solution is

$$ds^2 = -\left(1 - \frac{2m(r)}{r}\right) dt^2 + \left(1 - \frac{2m(r)}{r}\right)^{-1} dr^2 + r^2 (d\theta^2 + \sin^2\theta d\varphi^2) \quad , \quad (32)$$

divide it by ds^2 and use for the Lagrangian the definition $L = -1$ [24], which leads to

$$1 = \left(1 - \frac{2m(r)}{r}\right) \dot{t}^2 - \left(1 - \frac{2m(r)}{r}\right)^{-1} \dot{r}^2 - r^2 (\dot{\theta}^2 + \sin^2\theta \dot{\varphi}^2) \quad , \quad (33)$$

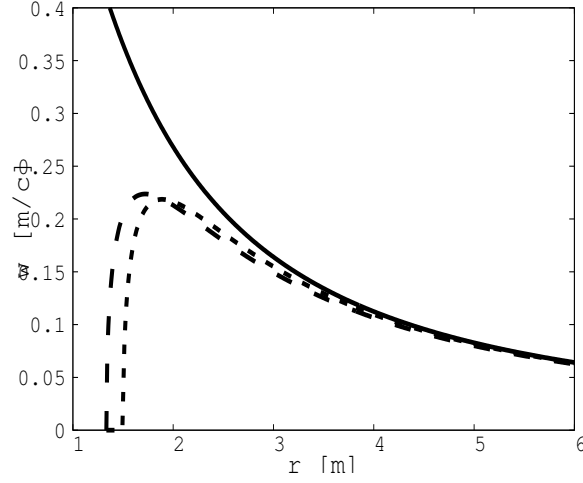


Figure 2: The angular frequency of a particle in a circular orbit, as a function in the radial distance and for $a = 0.95m_0$. The upper curve is the result as obtained within GR and the two lower curves within pc-GR. The curve with the maximum to the left is for $n = 3$ and the other one for $n = 4$.

where the dot refers to the derivative in s . Using the angular momentum conservation $l = r^2\dot{\varphi} = \text{const}$, that the motion is in the plane of $\theta = \frac{\pi}{2}$ and that $\left(1 - \frac{2m(r)}{r}\right)\dot{t} = h = \text{const}$ (which is the result of the variation with respect to the time), we arrive at

$$1 = \left(1 - \frac{2m(r)}{r}\right)^{-1} h^2 - \left(1 - \frac{2m(r)}{r}\right)^{-1} \dot{r}^2 - \frac{l^2}{r^2} . \quad (34)$$

Changing the derivative with respect to s to the one with respect to φ , leads to

$$r' = \frac{dr}{d\varphi} = \frac{\dot{r}}{\dot{\varphi}} \rightarrow \dot{r} = \dot{\varphi}r' = \frac{l}{r^2}r' , \quad (35)$$

where the prime now refers to the derivative with respect to φ .

Multiplying (34) by $\left(1 - \frac{2m(r)}{r}\right)$ and using (35), we arrive at the equation

$$\left(1 - \frac{2m(r)}{r}\right) = h^2 - \frac{l^2}{r^4}(r')^2 - \frac{l^2}{r^2} \left(1 - \frac{2m(r)}{r}\right) . \quad (36)$$

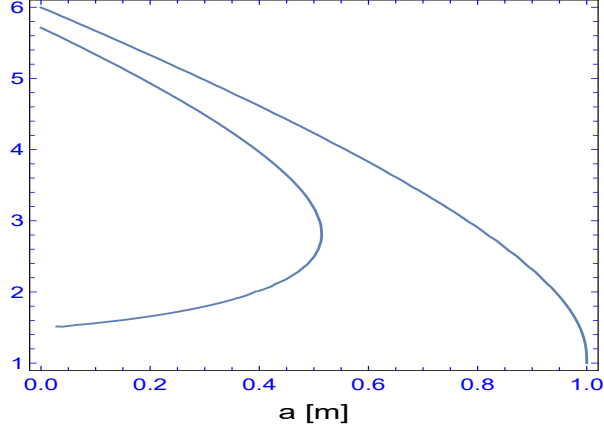


Figure 3: Limits of stable orbits within GR and pc-GR ($n = 4$). The upper curve is for GR, and the inner curve for pc-GR. Below the upper curve, no stable orbits exist, while in pc-GR no stable orbits exist to the left of the inner curve. Thus, in pc-GR, for a -values to the right of the inner curve all orbits are stable.

Next, the variable r is changed to u , namely

$$r = \frac{1}{u} \rightarrow r' = -\frac{u'}{u^2} . \quad (37)$$

Substituting this into (36) and resolving for $(u')^2$, one arrives at

$$(u')^2 = \frac{(h^2 - 1)}{l^2} + \frac{2m(u)}{l^2}u - u^2 + 2m(u)u^3 , \quad (38)$$

where $m(u)$ is given by

$$m(u) = m_0 \left(1 - \frac{27}{32} m_0^3 u^3 \right) . \quad (39)$$

In the next steps, (38) is again derived with respect to φ and the resulting equation is divided by $2u'$, arriving finally at the equation

$$u'' + u = \frac{m_0}{l^2} + 3m_0 u^2 - \frac{27}{8} \frac{m_0^4}{l^2} u^3 - \frac{81}{16} m_0^4 u^5 . \quad (40)$$

Define the small number $\varepsilon = 3m_0A$, which is for the solar system of the order of 10^{-7} [36], where $A = \frac{m_0}{l^2}$ is the areal velocity on the planetary plane. With this, the m_0 can be set equal to $\frac{\varepsilon}{3A}$ and (40) can be rewritten as

$$u'' + u = A + \frac{\varepsilon}{A}u^2 - \frac{A}{8} \left(\frac{\varepsilon}{A}\right)^3 u^3 - \frac{1}{16} \left(\frac{\varepsilon}{A}\right)^4 u^5 \quad . \quad (41)$$

In the first line, the first term on the right hand side is the classical, Newtonian contribution, while the second term is the standard relativistic correction which leads to the known perihelion shift of Mercury. The terms in the second row are explicit new contributions from pc-GR, however of order ε^3 . Thus, new contribution of pc-GR are at least two order of magnitude less, the one of order ε^2 coming only from GR (implicitly contained in the term $\frac{\varepsilon}{A}u^2$ when u is also expanded in ε). Thus, there is no hope to detect these deviations. This result also shows that GR and pc-GR are indistinguishable from each other in solar system observations. Still, this calculation is an interesting exercise, which might be of relevance when the perihelion shift of objects very near to a super-massive black hole is observed.

4.3 Quasi Periodic Objects

We mention shortly a former discussion on so-called *Quasi-Periodic objects*. There are several kinds, but here we refer to bright light emissions in accretions discs with a near periodic time dependence. At first, this phenomenon was associated to a bright spot which is co-moving with the accretion disc, thus, appearing and fading away from the observer as it turns around the black hole. Such events were observed [17, 37, 38, 39, 40, 41] in black hole binaries, but also exist in central black holes of galaxies. The GR can provide an estimation their distance to the center of the black hole, using the dependence in r of the orbital period of a circular particle. In order to confirm this distance, the redshift of the emission line has to be measured, too, which depends on r . The radial distance deduced from the orbital frequency and the redshift have to coincide for consistency. For central black holes the redshift has not been observed yet, but it is for stellar black holes.

The assumption is that the QPOs are the result of a bright spot moving around the black hole, which is obvious for black holes in the center of galaxies. However, for stellar black holes there may be a distinct mechanisms, like oscillations provoked by the companion star, as suggested in [42]. Thus, GR can still be saved. The question remains: Why the interpretation of OPOs should be different from the ones in the accretion disc of a black holes in the center of a galaxy? We argue that the same mechanism should also hold for stellar black holes, at least dominantly.

In order to understand the motion of a point-particle around a black hole, we resume some fundamental properties of this particle in a circular orbit: In Fig. 2 the dependence of the orbital frequency as a function in r is depicted for the rotational Kerr-parameter $a = 0.95m_0$. The upper curve is the result for GR, while in the lower curve the one for pc-GR is plotted. In GR the curve shows a steady increase of the orbital frequency, contrary to pc-GR which predicts a maximum, after which it falls off again.

Deducing a distance from the orbital period and from the redshift, leads for $n = 3$ to Fig. 4, where the observation is compared to the theory, using the a -parameter deduced. The zero is for $n = 3$ at $r = \frac{4}{3}m_0$ and for $n = 4$ to $r = \frac{3}{2}$, which are practically indistinguishable within the plot, i.e., the consequences are the same.

There is a great mismatch between the distance deduced from the orbital frequency and the redshift, using GR. In pc-GR, however, the results agree. A simple explanation leads to an agreement to observation! Nevertheless, because GR can be still reconciled, though, via a more complex explanation, nothing can be decided up to now.

4.4 Accretion disc structure

In order to understand the predicted light emission from an accretion disc in pc-GR, stable circular orbits have to be discussed: In Fig. 3 the last stable orbit (or ISCO for *Innermost Stable Circular Orbit*) as a function in a is shown. In GR the ISCO starts at $6m_0$ and is lowered to $r = m_0$ for $a = 1$. Below the upper line in Fig. 3 no stable orbit exists. This is different in pc-GR: The lower curve shows the limits of stable orbits, where to its left no stable orbit exists but to its right it does. The curve turns at about $a = 0.5m_0$, thus above $a = 0.5m_0$ all orbits are stable. It is this region where they can reach the maximum of the orbital frequency, below this value of a they don't.

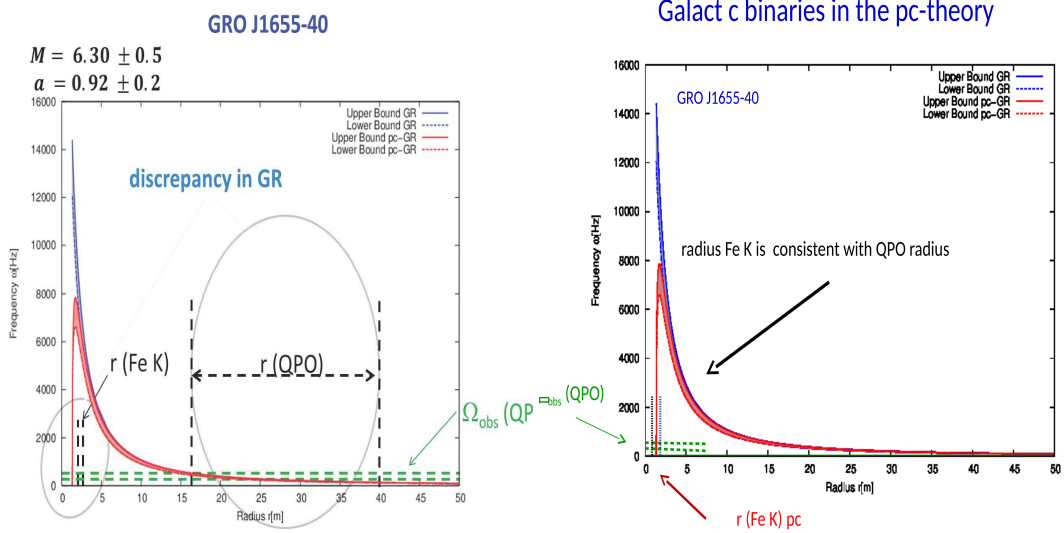


Figure 4: *Quasi-Periodic Objects* (QPO) compared to GR and pc-GR. The upper curve corresponds to the orbital frequency deduced within GR, where the thickness of the line indicates the resolution of the observation. The lower curve corresponds to pc-GR for $n = 3$. For $n = 4$ the differences are minor, which is the reason no new calculations were performed. The horizontal dashed lines show the observed orbital frequency with the experimental error, while the vertical lines show the deduced radial distance from the redshift of the $K\alpha$ -line.

For small a , the curve for pc-GR follows neatly the one of GR. Thus, we do expect a similar emission profile structure, except for the intensity of the light emitted, because the curve is further into the gravitational well and more energy is released. When $a > 0.5m_0$ the stable orbits reach the maximum of the orbital frequency. At this maximum, neighboring orbitals have a similar frequency and the excitation of the disc is minimal, producing a dark ring. To resume, pc-GR provides a robust prediction of the emission profile with a dark ring follows further in by a small bright ring.

The structure of the emission on accretion discs is discussed in [43, 44], comparing GR with pc-GR, besides what happens when a cloud is approaching the black hole.

In Fig. 5 a simulation is shown, using the model published in [45], which assumes a thin, optical thick accretion disc. This is not a very realistic model, expecting rather a thick disc, maybe with the form of

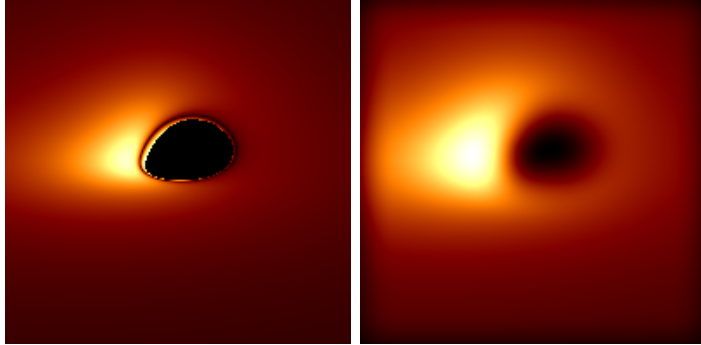


Figure 5: The simulations on the left and right panel are within pc-GR. The resolution on the left is for $5\mu\text{as}$ while on the right it is for $20\mu\text{as}$. The inclination angle with respect to the observer is 70° . Clearly seen is that the ring structure, as predicted by pc-GR, is washed out, showing that the EHT observation cannot discriminate between pc-GR and GR.

a torus. For such discs, other models are better suited, from which we just mention one, namely [46]. Nevertheless, the emission structure is robust and should be similar in all disc models, changing only the absolute value of the intensity emitted.

On the left hand side of Fig. 5 the result for a high resolution is depicted, while the right hand side shows the result for a low resolution of $20\mu\text{as}$. For the low resolution case, the ring structure is unfortunately lost. The *Event Horizon Telescope* (EHT) [4, 5, 6, 7, 8, 9], which observed the shadow of the central black hole of M87, has a resolution of only $24\mu\text{as}$, which is too low to dissolve the ring structure. Therefore, one has to wait for future observations with an improved resolution. Note that the EHT is not able to distinguish between GR and different kinds of extensions

The disc model used by EHT consists of an optical thin plasma surrounding the black hole (see also [47]). This is only one of many possible disc models, most of which are optical thick. The shadow is simulated tracing the most inner photon (or Einstein) rings. While in GR for $a = 1m_0$ all photon rings are blocked by a optical thick accretion disc, because the ISCO reaches $r = m_0$, in pc-GR all photon rings are blocked, because for $a > 0.5m_0$ all orbits are stable until to the surface of the star. A definite answer can only be given, when the disc is proven to be optical thin and/or pc-GR is confirmed or not.

4.5 Cosmology: The Robertson-Walker Model

The pc-Robertson-Walker metric was introduced in [48] and can also be retrieved from [17]. The length element is given by

$$d\omega^2 = (dX^0)^2 - \frac{a(t)^2}{\left(1 + \frac{ka(t)^2}{4a(0)^2}\right)^2} d\Sigma^2, \quad (42)$$

where $d\Sigma^2$ is the angular volume element, $a(t)$ is the radius of the universe, $a(0)$ its value at present time (set to 1) and k is a parameter, which only for $k = 0$ corresponds to a flat universe [36, 49]. This value will be used from here on, because all observational data suggest a flat universe.

For the energy-momentum tensor an isotropic fluid is assumed, i.e.,

$$(T^\mu_\nu) = \begin{pmatrix} \rho & & & \\ & -\frac{p}{c^2} & & \\ & & -\frac{p}{c^2} & \\ & & & -\frac{p}{c^2} \end{pmatrix}, \quad (43)$$

Using the metric (42), the y_μ can be determined, using the differential equation (26). Because an isotropic universe is assumed, the development of the radius $a(t)$ is the same in any direction. Therefore, it suffices to define y_μ as $a_I(t)$.

In analogy to (28) and using $a(t) = a_R(t) + I a_I(t)$, we arrive at

$$\begin{aligned} \frac{da_I}{da_R} &= \frac{\left[\frac{(a_R(t)-a_I(t))^2}{a(0)^2} - \frac{(a_R(t)+a_I(t))^2}{a(0)^2}\right]}{\left[\frac{(a_R(t)-a_I(t))^2}{a(0)^2} + \frac{(a_R(t)+a_I(t))^2}{a(0)^2}\right]} \\ &= -4 \frac{a_R a_I}{a_R^2 + a_I^2}. \end{aligned} \quad (44)$$

Because the a_I has to be very small compared to a_R , we obtain approximately, setting $a(0) = 1$,

$$\frac{da_I}{da_R} = -4 \frac{a_I}{a_R}. \quad (45)$$

Separating variables and integrating, we finally obtain

$$a_I = A \frac{1}{a_R^4} . \quad (46)$$

Demanding an a_I proportional to $\dot{a}_R(0)$ at $t = 0$, as similarly done in the Schwarzschild case, we can set $A = \dot{a}_R(0)$. Thus, today $a_I(0) = \dot{a}_R(0)$ (compared to $a_R(0) = 1$), which is extremely small, and it continues to be even smaller for larger times. However, for $t \rightarrow 0$ (time of the Big Bang), the a_I explodes and becomes infinite very near to the big bang, implying a dominance of the dark energy. Of course, in this case, the approximation of a small a_I , compared to a_R is not valid anymore, but the results enlightens the *tendency* of a strong increase of $a_I(t)$. Apart from that, very near to the big bang the mass/energy density is extremely high and according to our assumption additional vacuum fluctuations building up (see section 4.6).

In [17, 48] the possible fates of the universe were determined. The equations of motion were set up and the differential equation for the second derivative of a_R became, assuming that the matter distribution in the universe behaves as dust,

$$\frac{a_R''}{\frac{4\pi G}{3}} = (3\beta - 1)\Lambda a_R^{3(\beta-1)+1} - \varrho_0 a_R^{-2} , \quad (47)$$

where ϱ_0 is the matter density at the present date. The β is a parameter of the dark energy density $\varrho_\Lambda = \Lambda a_R^{3(\beta-1)}$. For $\beta = 1$ this energy density is just Λ , as it seems to be satisfied today. G is the gravitational constant.

With this, the differential equation of the radius of the universe is

$$\frac{a_R''}{\frac{4\pi G}{3}\varrho_0} = 2\Lambda a_R - a_R^{-2} . \quad (48)$$

The acceleration starts with a negative sign in the early epoch of the universe until $a_R'' = 0$, which is reached when $a_R = 1/(2\Lambda)^{\frac{1}{2}}$, after which the acceleration becomes positive, as observed today.

In [17, 48] also other scenarios were discussed, taking different values of β . As a result, besides a rip-off for values $\beta > 1$, also solutions were found, which for $t \rightarrow \infty$ approaches a constant value or even a zero positive acceleration (0_+).

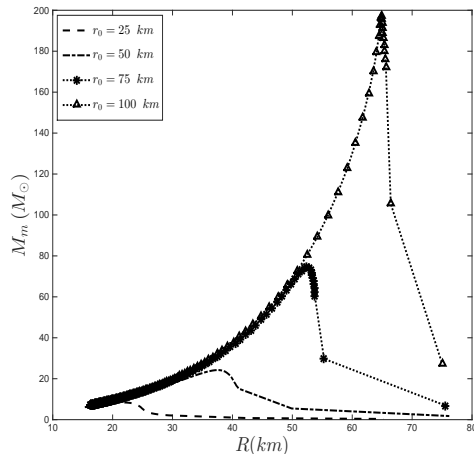


Figure 6: Within pc-GR, stable stars up to 200 solar masses are obtained for a coupling of the dark energy density to the mass density, which diminishes approaching the surface.

4.6 Neutron stars

The pc-GR conjectures that there is no event horizon, implying that all so-called black holes are rather gray stars, even when they have a mass billion times more than the sun. The question is, if one can describe the internal structure of such stars and explain their stability. One problem is that there is no such theory, because no one can deduce the equation of state under such extreme mass densities. However, one can try to extrapolate from low masses to larger ones, using recently developed theories for neutron stars. Such a theory is published in [50], which is a mean-field approach involving different hadron states including strange hadron fields.

In [51, 52] this mean-field model was coupled to dark energy within the star. As a first approximation, a linear coupling between the dark energy density to the mass density was assumed:

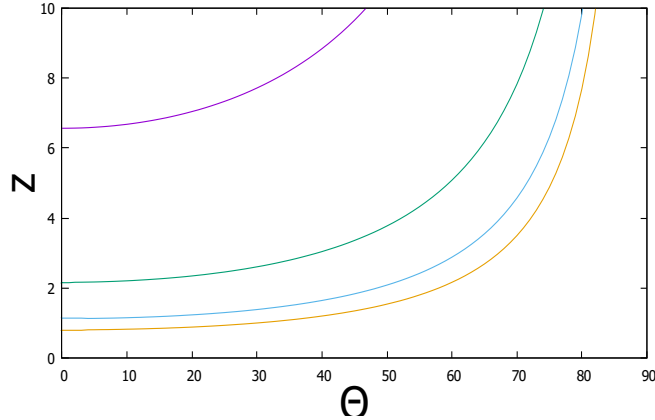


Figure 7: The redshift at the surface $r = \frac{3}{2}m_0$ as a function of the azimuthal angle θ , for different a -values. From top to bottom, the curves correspond to $0.2m_0$, $0.5m_0$, $0.8m_0$ to $1.0m_0$.

$$q_\Lambda = \alpha q_m \quad , \quad (49)$$

with the result of up to 6 solar masses already found to be stable. This is interesting in view of recent attempts to explain higher neutron masses [53] due to the possible detection of a neutron star with 2.6 solar masses in a gravitational wave event [54]. *This is a hint that even larger neutron star masses can exist*, though, it should be expected that their internal structure has to change significantly.

No higher masses could be obtained, because the linear coupling resulted in a repulsion effect shedding off mass from the star for increasing mass. This was the motivation to reanalyze vacuum fluctuations within the star, using semi-classical Quantum Mechanics, as explained in [26]. In [55] the monopole approximation [56] was used and the coupling between the dark energy and mass density deduced. As a result a decrease of the coupling near the surface was obtained and stable solutions of up to 200 solar masses were obtained, see Fig, 6. This presented at the same time a limit due to the end of validity of the mean-field theory [50]. For higher masses other, not yet developed theories have to be searched for.

How one could detect such large neutron stars (if one can still denote them as neutron stars is a big question, too)? One possibility

is to look for emissions from infalling matter and/or beams emitted as in standard neutron stars. This is not as easy, because near the position of the so-called event horizon the redshift is extremely large, at least in the orbital plane. This is illustrated in Fig, 7, where the redshift at $r = \frac{3}{2}m_0$ (which is the position of the event horizon for $a = 0$, with the mass-function used) is plotted versus the azimuthal angle θ , for a set of Kerr-rotational parameters a . As can be seen, near the poles the redshift is, for large values of a , of the order of 1. Thus, if a is near to 1, highly redshifted light emission may be seen near the poles, when matter falls in there. When, however, the so-called black hole has an accretion disc, there has to be a jet emerging near the poles, over-shining this effect. Hopefully, one can observe it in SgrA* which is believed to be devoid of an accretion disc.

It remains to be mentioned that in [57, 58] also neutron stars, as compact objects, were investigated within pc-GR from the viewpoint of an effective field theory. In [59, 60] the effects of dark matter within pc-GR were also investigated. All these contributions reflect a range of observable consequences and applications of pc-GR for neutron stars.

4.7 Gravitational waves

In 2016 the first observed gravitational wave event was reported in [2, 3]. Assuming that GR is the theory to describe the merger, a two-point approximation seems to be justified, mainly because the ISCO is still far away from contact. The steps for obtaining the *chirping mass* \mathcal{M}_c , using the two-point approximation, are explained in [61]. In [62] the same approximation was used, with the caveat that the two black holes can approach each other until their event-horizon touch each other, which renders the two-point approximation senseless. Nevertheless, this approach serves to extract trends on how the deduced chirping mass changes. The modified equation for the chirping mass is

$$\mathcal{M}_c = \widetilde{\mathcal{M}}_c F_\omega(\bar{r}) = \frac{c^3}{G} \left[\frac{5}{96\pi^{\frac{8}{3}}} \frac{df_{\text{gw}}}{dt} f_{\text{gw}}^{-\frac{11}{3}} \right]^{\frac{3}{5}}, \quad (50)$$

where on the right hand side values of the observed frequency and its change in time appears. The left hand side contains the modified chirping mass $\widetilde{\mathcal{M}}_c$ and the apparent chirping mass \mathcal{M}_c , the number deduced in [2, 3]. Both are related by a factor $F(R)$, where R is the relative distance of the two black holes. In the calculation it is

assumed that the mass of both is approximately equal as it was in the observed case. $n = 3$ was used, for which the function is given by $F_\omega(R) = \left(1 - \left(\frac{2R_S}{3R}\right)^2\right)$, where $R_S = 2m_0$ is the Schwarzschild radius of one of the black holes. For $n = 4$ the new expression is $F_\omega(R) = \left(1 - \left(\frac{3R_S}{4R}\right)^3\right)$. In any case, the $F(R)$ tends to a small value until the touching configuration (twice the Schwarzschild radius for equal mass companions), implying that the real chirping mass is larger than the deduced one using GR- Here it is important to note that the approach to deduce the mass in [2, 3] is *theory dependent*, as it is also in pc-GR. In pc-GR a larger mass should result and, thus, also the luminosity distance has to be larger, such that the same is observed on Earth. How large, depends very much on the model used to describe the inspiral phase. A simple two-point approximation does not work and one needs more sophisticated methods, as for example a numerical relativistic hydrodynamical approach [63].

In contrast, it is much easier to describe the ring-down modes of a black hole, i.e., after the two black holes have merged. The ring-down modes are obtained investigating the stability of the final black hole under metric perturbations. For the Schwarzschild case, this part is well described in the book by S. Chandrasekhar [64], which can be directly extended to the pc-GR metric. There are two types of modes, the negative parity solutions, also called Regge-Wheeler modes [65], and the positive parity modes, also called Zerilli modes [66]. In [67] the axial modes were calculated for $n = 3$ and in [68] also the axial modes were calculated, now for $n = 4$. The time dependence of the ring-down modes is $e^{-i\omega t} = e^{-i\omega_R t} e^{\omega_I t}$, with $\omega = \omega_R + i\omega_I$, separated in its real and imaginary part. For damped modes the $-\omega_I$ has to be positive.

The Regge-Wheeler equation is solved as explained in [67, 68], using an iterative technique called the *Asymptotic Iteration Method* (AIM) [69], and in Fig. 8 the result for small $-\tilde{\omega}_I$ is depicted (we defined $\tilde{\omega} = m_0\omega$). Note that there are no unstable modes with negative $-\tilde{\omega}_I$. The real part of then frequencies is in general slightly larger than in GR, however, without any possibility to discriminate between GR and pc-GR. Also the iteration number is yet too low for going to larger values of $-\tilde{\omega}_I$.

However, which modes will be excited depends very much on the dynamics in the inspiral phase. Our suggestion is to use the numerical method as described in [63], changing in the programs the metric of

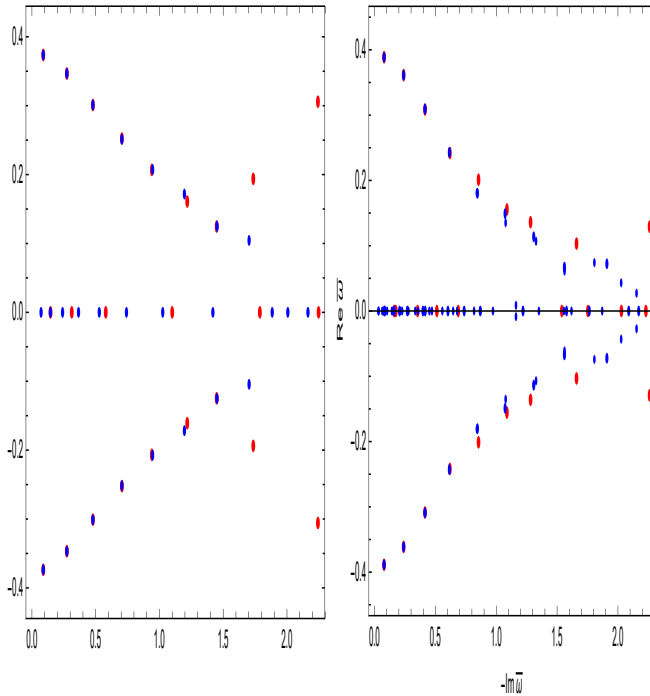


Figure 8: Axial gravitational modes within GR (left panel) and pc-GR (within pc-GR). The iteration number is 20 (red dots) and 40 (blue dots), using the *Asymptotic Iteration Method* [69].

GR to the one of pc-GR.

The polar modes present some practical problems, rendering it more difficult to solve. This will be addressed in a future publication.

5 Conclusions

A review was presented on the consequences of the *pseudo-complex General Relativity* (pc-GR), comparing the results with GR. In general, differences are only visible near massive objects of the size of a black hole, requiring however a large resolution

The pc-GR is an algebraic extension of GR, where the coordinates x^μ are redefined to $X^\mu = x^\mu + Iy^\mu$. This modifies the Einstein equations with a dark energy energy momentum tensor on its right hand side. This tensor depends of u_μ and \dot{y}_μ . Demanding a real length element, a differential equation for y_μ was obtained. The y_μ are pro-

portional to the 4-velocity, multiplied with the scalar minimal length parameter. The y_μ was determined for the pc-Schwarzschild case and the pc-Robertson-Walker universe.

Observational consequences of pc-GR were determined, as the appearance of a dark ring, followed by a bright inner ring, in the light emission of an accretion disc. Unfortunately the resolution of the EHT is too low for seeing this structure, thus, it cannot discriminate between GR and pc-GR.

Modification in the perihelion shift of Mercury were discussed, with the result that pc-GR only adds corrections of 10^{-14} to the shift calculated within GR, i.e., no hope to being seen.

Also *Quasi Periodic Objects* were discussed and interpretations within GR and pc-GR were compared, without a definitive result.

Neutron stars of any mass were obtained, though, for large masses the star rather resembles the one of a black hole. It is suggested to look for light emission of infalling matter at the poles, being excited upon impact, provided there is no jet emitted nearby. At the poles the minimal redshift is of the order of 1, increasing rapidly to infinity at the orbital plane.

The Robertson-Walker universe gives in practice the same results as in GR for the present epoch and later times. In the limit of $t \rightarrow 0$, however, the dark energy increases significantly, implying an important role of it at early times.

As a last example, gravitational waves from the ring-down of a black hole were also discussed, indicating similar results as in GR. For large damping modes, the real part of the frequencies are larger in pc-GR than in GR.

Acknowledgments

This work was supported by DGAPA-PAPIIT (IN100421). Very useful discussions with Laurent R. Loinard (IRyA, UNAM) are also acknowledged.

References

- [1] C. M. Will, The confrontation between general relativity experiment, *Living Rev. Relativ.* **9** (2006), 3.

- [2] Abbott B. P. et al. (LIGO Scientific Collaboration and Virgo Collaboration), Observation of Gravitational Waves from a Binary Black Hole Merger, *Phys. Rev. Lett.* **116** (2016), 061102.
- [3] Abbott B. P. et al. (LIGO Scientific Collaboration and The Virgo Collaboration), GW151226: Observation of Gravitational Waves from a 22-Solar-Mass Binary Black Hole Coalescence, 2016c, *Phys. Rev. Lett.* **116**, 241103.
- [4] The Event Horizon Telescope collaboration, First M87 Event Horizon Telescope Results. I. The Shadow of the Supermassive Black Hole, *ApJ* **875** (2019), L1.
- [5] The Event Horizon Telescope collaboration, First M87 Event Horizon Telescope Results. II. Array and Instrumentation, *ApJ* **875** (2019), L2.
- [6] The Event Horizon Telescope collaboration, First M87 Event Horizon Telescope Results. III. Data Processing and Calibration, *ApJ* **875** (2019), L3.
- [7] The Event Horizon Telescope collaboration, First M87 Event Horizon Telescope Results. IV. Imaging the Central Supermassive Black Hole, *ApJ* **875** (2019), L4.
- [8] The Event Horizon Telescope collaboration, First M87 Event Horizon Telescope Results. V. Physical Origin of the Asymmetric Ring, *ApJ* **875** (2019), L5.
- [9] The Event Horizon Telescope collaboration, First M87 Event Horizon Telescope Results. VI. The Shadow and Mass of the Central Black Hole, *ApJ* **875** (2019), L6.
- [10] A. Einstein, A Generalization of the Relativistic Theory of Gravitation, *Ann. Math.* **46** (1945), 578.
- [11] A. Einstein, A Generalized Theory of Gravitation, *Rev. Mod. Phys.* **20** (1948), 35.
- [12] M. Born, A suggestion for unifying quantum theory and relativity, *Proc. Roy. Soc. A* **165** (1938), 291.
- [13] M. Born, Reciprocity Theory of Elementary Particles, *Rev. Mod. Phys.* **21** (1949), 463.
- [14] E. R. Caianiello, Is there a maximal acceleration?, *Il Nuovo Cim. Lett.* **32** (1981), 65.

- [15] E. R. Caianiello, Maximal acceleration as a consequence of Heisenberg's uncertainty relation, *Il Nuovo Cim. Lett.* **41** (1984), 370.
- [16] P. O. Hess, W. Greiner, Pseudo-complex General Relativity, *J. Mod. Phys. E* **18**, 51 (2009).
- [17] Hess P. O., Schäfer M., Greiner W., *Pseudo-Complex General Relativity*; Springer: Heidelberg, Germany, 2015.
- [18] K. Becker, M. Becker, J. Schwarz, *String Theory and M-Theory: A Modern Introduction*, (Cambridge University Press, Cambridge, 2007).
- [19] L. Smolin, *Three Roads to Quantum Gravity*, (Basic Books, New York, 2001).
- [20] P. F. Kelly, R. B. Mann, Ghost properties of algebraically extended theories of gravitation, *Class. and Quant. Grav.* **3**, 705 (1986).
- [21] P. O. Hess, Review on the pseudo-complex General Relativity and Dark Energy, *High Energy Physics* **2019** (2019), 1840360.
- [22] P. O. Hess, Alternatives to Einstein's General Relativity Theory, *Progress in Particle and Nuclear Physics* **114** (2020) 103809.
- [23] C. L. M. Mantz, T. Prokopex, Hermitian Gravity and Cosmology, arXiv:gr-qc/0804.0213
- [24] T. Schönenbach, G. Caspar, P. O. Hess, T. Boller, A. Müller, M. Schäfer, W. Greiner, Experimental tests of pseudo-complex General Relativity, *MNRAS* **430** (2013), 2999.
- [25] T. Schönenbach, G. Caspar, P. O. Hess, T. Boller, A. Müller, W. Greiner, Ray-tracing in pseudo-complex General Relativity, *MNRAS* **442** (2014), 121–130.
- [26] N. D. Birrell and P. C. W. Davies, *Quantum Fields in Curved Space* (Cambridge University Press, The Edinburgh Building, Cambridge, 1994).
- [27] M. Visser, Gravitational vacuum polarization. II. Energy conditions in the Boulware vacuum, *Phys. Rev. D* **54** (1996) 5116.
- [28] A. Nielsen, O. Birnholz, Testing pseudo-complex general relativity with gravitational waves, *AN* **339** (2018), 298.
- [29] A. Nielsen, O. Birnholz, Gravitational wave bounds on dirty black holes, *AN* **340** (2019), 116.

- [30] A. Feoli, G. Lambiase, G. Papini, G. Scarpetta, Schwarzschild field with maximal acceleration corrections, *Phys. Lett. A* **263** (1999), 147.
- [31] F. P. Schuller, Born–Infeld kinematics and correction to the Thomas precession *Phys. Lett. B* **540** (2002), 119.
- [32] F. P. Schuller, Born–Infeld Kinematics, *Ann. Phys. (N.Y.)* **299** (2002), 174.
- [33] F. P. Schuller, *Dirac-Born-Infeld kinematics, maximal acceleration and almost product manifolds*, Ph.D. thesis, University of Cambridge (2003).
- [34] F. P. Schuller, M. N. R. Wohlfarth, T. W. Grimm, Pauli–Villars regularization and Born–Infeld kinematics, *Class. Quant. Grav.* **20** (2003) 4269.
- [35] MATHEMATICA 11.3.0.0. 2018, Wolfram Research Foundation.
- [36] R. Adler, M. Bazin and M. Schiffer, *Introduction to General Relativity*, (McGraw-Hill, New York, 1975).
- [37] P. O. Hess, W. Greiner, Pseudo-complex General Relativity: Theory and observational consequences”, in *Centennial of General Relativity: A Celebration*, text-book edited by Cesar Zen, World Scientific, 3. chapter, (2017). p. 97.
- [38] T. H. Belloni, A. Sanna, M. Mendz, High-frequency quasi-periodic oscillations in black hole binaries, *MNRAS* **426** (2012), 1701.
- [39] R. T. Hynes, D. Steeghs, J. Casares, P. A. Charles, K. O’Brian, The Distance and Interstellar Sight Line to GX 339–4, *ApJ* **609** (2004), 317.
- [40] R. C. Reis, A. Fabian, R. R. Ross, G. Miniutti, J. M. Miller, C. Reynolds, A systematic look at the very high and low/hard state of GX 3394: constraining the black hole spin with a new reflection model, *MNRAS* **387** (2008), 1489.
- [41] J. Steiner, J. McClintock, G. Jeffrey et al., Deriving the spins of accreting stellar-mass black holes from their X-ray continuum spectra, 38th COSPAR Scientific Assembly, 18–15 July, Bremen, Germany, 2010).
- [42] D. Lai, W. Fu, D. Tsang, J. Horak, C. Ya, High-Frequency QPOs and Overstable Oscillations of Black-Hole Accretion discs, 2012, *Proc. of the Intern. Astron. Union* **290** (2012), 57.

- [43] Th. Boller, P. O. Hess, H. Stöcker and A. Müller, "Predictions of the pseudo-complex theory of gravity for EHT observations – I. Observational tests", *MNRAS:Letters* **485** (2019), L34-L37.
- [44] P. O. Hess, Th. Boller, H. Stöcker and A. Müller, "Predictions of the pseudo-complex theory of Gravity for EHT observations-II. Theory and predictions", *MNRAS:Letters* **485** (2019), L121-L125.
- [45] D. N. Page, K. S. Thorne, disc-Accretion onto a Black Hole. Time-Averaged Structure of Accretion disc, *ApJ* **191** (1974), 499.
- [46] W. Kluzniak, and S. Rappaport, Magnetically Torqued Thin Accretion discs, *ApJ* **671** (2007), 1990.
- [47] M. D. Johnas, et al., Universal Interferometric signatures of a black hole's photon ring, arXiv:1907.04329[at-oh-ph]
- [48] P. O. Hess, L. Maghlaoui, W. Greiner, The Robertson-Walker metric in a pseudo-complex General Relativity, *Int. J. Mod. Phys. E* **19** (2010), 1315.
- [49] C. W. Misner, K. S. Thorne and J. A. Wheeler. *GRAVITATION*, (H. W. Freeman and Company, San Francisco, 1973).
- [50] V. Dexheimer, S. Schramm, Proto-Neutron and Neutron Stars in a Chiral SU(3) Model, *ApJ* **683** (2008) 943.
- [51] I. Rodríguez, P. O. Hess, S. Schramm, W. Greiner, Neutron stars within pseudo-complex general relativity, *J. Phys. G* **41**, (2014), 105201.
- [52] I. Rodríguez, PhD thesis, *Neutron Stars within Pseudo-complex General Relativity*, Johann-Wolfgang von Goethe Universität, Frankfurt am Main (2014).
- [53] J. E. Horvath, L. S. Rocha, A. Bernardo, R. Valentim and M. G. B. de Avellar, *AN* (2021) in press.
- [54] R. Abbott et al., *The Astroph. J. Letters* **896** (2020), L44.
- [55] G. Caspar, I. Rodríguez, P. O. Hess, W. Greiner, Vacuum fluctuation inside a star and their consequences for neutron stars, a simple model, *Int. J. Mod. Phys. E* **25** (2016), 1650027.
- [56] T. Padmanabhan, Gravity and the Thermodynamics of Horizons, *Phys. Rep.* **406** (2005) 49.
- [57] G. L. Volkmer, *Um Objeto Compacto Excótico na Relatividade Geral Pseudo-Complexa*", PhD thesis, Porto Alegre, March 2018.

- [58] M. Razeira, D. Hadjimichef, M. T. V. Machado, F. Köpp, G. L. Volkmer, C. A. Z. Vasconcellos, Effective field theory for neutron stars with WIMPS in the pc-GR formalism, *AN* **338** (2017), 1073.
- [59] D. Hadjimichef, G. L. Volkmer, R. O. Gomes and C. A. Z. Vasconcellos, Dark Matter Compact Stars in Pseudo-Complex General Relativity, *Memorial Volume: Walter Greiner*, eds. P. O. Hess and H. Stöcker, (World Scientific, Singapore, 2018).
- [60] G. L. Volkmer, D. Hadjimichef, Mimetic Dark Matter in Pseudo-Complex General Relativity, *Int. J. Mod. Phys.: Conf. Series* **45** (2017), 1760012.
- [61] M. Maggiore, *Gravitational Waves*, (Oxford University Press, Oxford, 2008).
- [62] P. O. Hess, The black hole merger event GW150914 within a modified theory of general relativity, *MNRAS* **462** (2016), 3026.
- [63] L. Rezzolla and O. Zanotti, *Relativistic Hydrodynamics*, (Oxford University Press, Oxford, UK, 2013)
- [64] S. Chandrasekhar, *The Mathematical Theory of Black Holes*, (Clarendon Press, Oxford, 1983).
- [65] T. Regge, J. A. Wheeler, Stability of a Schwarzschild Singularity, *Phys. Rev.* **108** (1957), 1063.
- [66] F. J. Zerilli, Effective Potential for Even-Parity Regge-Wheeler Gravitational Perturbation Equations, *Phys. Rev. Lett.* **24** (1970), 737.
- [67] P. O. Hess, E. López-Moreno, Regge–Wheeler and Zerilli equations within a modified theory of general relativity, *Astr. Nachr.* **340** (2019), 89.
- [68] P. O. Hess, E. López-Moreno, Axial ring down modes in General Relativity and in its pseudo-complex extension, *Astr. Nachr.* (2020), in press.
- [69] H. Cho, A. S. Cornell, J. Doukas, T.-R. Huang and W. Naylor, *Adv. in Math. Phys.* **2012** (2012), 281705.